ORIENTAL JOURNAL OF CHEMISTRY
An International Open Access, Peer Reviewed Research Journal
www.orientjchem.org
ISSN: 0970-020 X
CODEN: OJCHEG
2025, Vol. 41, No.(4):
Pg. 1277-1284

Thermal Analysis of Copper Metal Complexes: Insights from TGA and DSC

DHARA D. PATEL[1]*, K. R. PATEL[2], K. P. PATEL[3] and V. D. PATEL[4]

[1]Department of Chemistry, Sankalchand Patel University, Visnagar, Gujarat, India.
[2]Sheth. M. N. Science College, Patan, Gujarat, India.
[3]R.R.Mehta College of Science, Palanpur, Gujarat, India.
[4]Municipal Arts and Urbaan Bank Science College, Mehsana, Gujarat, India.
*Corresponding author E-mail: dr.dhara29@gmail.com

http://dx.doi.org/10.13005/ojc/410424

(Received: April 02, 2025; Accepted: July 12, 2025)

ABSTRACT

The nature and content of Metal and Ligand have a significant impact on the behavior and properties of Metal Complexes. Metal Cu(II) with Ligands, 2-Methyle Amine(2-MA), P-Dimethyle Amine Benzaldehyde (PDAB) and Di(2-pyridyl)amide (DPA) were used to synthesized Metal Complexes. Author synthesized three ternary metal complexes typeMLxLyfor scientific investigation. In the current paper, thermal behavior using TGA of all the metal complexes were studied and discussed in details. The derivatives data were created to analyze the thermogram properly. The thermodynamics parameters were also determined with Broido method. Parameters such as Activation Energy Enthalpy, Entropy and Gibbs energy were computed from the TGA data using Broido method. The dynamic temperature aspect has been considered eventually and the results were presented in respective section. The DSC measurements curve illustrates heat flow with rising temperature. Specific heat, Heat, Heat Capacity and thermal diffusivities of complexes were measured form the analytical data. The investigation peak and region corresponding to enthalpy involved in the process has been identified in schematic DSC curve. Present investigation deals with measurement of the various thermal parameters of metal complexes besides some other thermal event measurement briefly discussed at room temperature to decomposition temperature.

Keywords: Thermogravitometric analysis, Differential scanning calorimetry, Activation energy, Enthalpy, Entropy, Specific heat.

INTRODUCTION

A lot of studies have been utilized to understand thermal dilapidation of metal complexes formed by 2-Ligands with d-block metal, with various metal concentrations, analyzed,using thermo-gravimetric analysis in a nitrogen(N) atmosphere from room temperature to 1000°C.[1–3] Various scientist also studied Differential Scanning Calorimetry investigationof metal complexes and resulting various thermal parameters[4–6]. A theoretical approach to the TGA actions of anseamless reaction is relatively straightforward. However, significant complications exist, and many analytical approaches have been suggested to gain kinetic-parameters from TGA statistics[7]. Cu(II) and Co(II)

complexes were produced with three azo group-containing Schiff base ligands. These constituents were examined using various physicochemical and spectroscopic systems, including (C,H,N,S) elemental-analysis, spectroscopy (FTIR, UV-Vis), magnetic-moment measurements, thermo-gravimetric analysis,and DSC.[8] Withinfrared(IR), (DSC) differential scanning calorimetry, and (TGA) thermo-gravimetric analysis,researchers examined the dealings and thermalactions of the poly (4-vinylpyridine-co-divinylbenzene)Cu(II) complex[9]. Complexes of divalent transition metal ions Cu(II) andCo(II) with ligand Aminobenzohydrazide and 2-mercaptobenzthiazole have been synthesized and characterized with TGA[10]. Some research compares and explains three distinct DSC approaches that are said to be used in the methodology in order to determine which is best for determining Cp[11]. During isothermal-cure, Cp may also be calculated by doing dynamic heating tests on a completely cured sample. For isothermal heat transfer models, which would ordinarily use a constant Cp value derived from the completely cured epoxy, such values are frequently enough[12].

Synthesis Method

The three different ligands such as 2-Methyle Amine(2-MA) as L_1 P-Dimethyle Amine Benzaldehyde(PDAB) as L_2 and Di(2-pyridyl) amide(DPA) as L_3 utilized to obtain three Schiff-base named L_1L_2, L_2L_3 and L_3L_1. The synthesis described by authors itself[13]. The stock solution of $CuCl_2$ was prepared. L_1(1.4919 g 0.1mol) solution in hot water was employed. L_2(1.0814 g 0.1mol) and L_3(1.237g 0.1mol) solution in ethanol were utilized. 50 mL of 100% ethanol was boosted to the L_1L_2, L_2L_3, and L_3L_1 mixture in a RBF, and the mixture was stimulated periodically for three hours. While placing the refluxed mixture in a cold bath, precipitates were produced. It was vacuumed, filtered, and distilled water washed. The accumulated Schiff bases have been preserved in a vacuum dessicator. The pure Schiff-bases were re-crystallized from absolute ethanol. By combining Schiff base (0.1mol) in hot ethanol solution with metal chloride salt solution (0.1mol) in distilled water, the metal complexes in crystal form developed. The metal solution was continuously stirred as the Schiff-base solution was gradually added. After being refluxed for two hours, the mixture was boiled for ten minutes to reduce the contents to half. After cooling, the crystals precipitated out. Filtered distilled water was used to wash the precipitates. All complexes were desiccated and dried before being stored.

Methodology

Thermogravimetric Analysis

The present work is considered as non-isothermal method to understand the thermal kinetic reaction. (TGA) and (DSC) were carried out using a Mettler Toledo and TA instrument . For both analyses, the heating rate was set to 10°C/min, and measurements were conducted over a temperature range of [e.g., 30–800°C] under a nitrogen atmosphere with a flow rate of 50 mL/minute. The sample mass used for each measurement was approximately 5–10 mg. Prior to analysis, the instruments were calibrated using standard reference materials: indium and zinc for DSC (based on their known melting points), and calcium oxalate for TGA. Calibration ensured accurate temperature and enthalpy measurements. The technique to evaluate the kinetic parameter in thermal analysis have been developed by Broido[7]. Auto catalyzed thermo set cure reactions are reaction products and catalyst for reactions that accelerateisothermal reaction rates as expressed by the Arrhenius Equation 1[14,15].

$$k = Ae(-Ea/RT) \quad (1)$$

Where, A = pre-exponential factor (1/s), Ea = activation energy (J/mol), R is universal gas constant (8.314J/mol.K), Tis temperature (K) and k is rate constant.

Thermogram of such a relationship reflects thisrate equation integrated from a temperature where *Yis* 1. According to Broido[7], the TG curve represents a raterelationship in which below Equation 2 is used to integrate atemperature at friction (y = 1) to reaction completion. The slope of the plot ln (ln 1/y) versus 1000/T isevaluted to find the activation energy as,

$$Ea = -2.303X\ RX\ Slope \quad (2)$$

Where, (R is gas constant).

The parameters, enthalpy($\Delta H\#$), entropy

(ΔS#) and Gibbs energy (ΔG#) of activation were calculated using the standard Equation-3, Equation-4 and Equation-5 respectively.

$$\Delta H = Ea - R\,Td \quad (3)$$

$$\Delta S = \left(\frac{\Delta H}{T}\right) - \left(\frac{4.576 \log T}{K}\right) - 47.22 \quad (4)$$

Where K'is –ln(ln 1/y)

$$G = \Delta H - T\Delta S. \quad (5)$$

Specific Heat Treatment

In the present DSC analysis we measured the heatcapacity Cp and kinetically hindered components[15] of the response according to Equation 6.

$$\frac{dQ}{dt} = C_P \frac{dT}{dt} + f(t,p) \quad (6)$$

Where, dQ/dt is total heat flow, dT/dt is temperature scanning rate with Cp. dT/dt representing the reversing signal and f(t,T) is function of time and temperature which depicts thermal processes that are kinetically regulated, such the process of enthalpy release, which is shown in the nonreversing signal.

Specific heat capacity is an aspect of thermal inertia since it shows how resistant a substance is to changes in temperature. In connection to the amount of heat Q, specific heat capacities at constant pressure(Cp) and at constant volume (Cv) are also can be calculated by Equation 7 and Equation 8 respectively[16].

$$C_p = \frac{Q}{m\Delta T} \quad (7)$$

$$C_v = C_p - R \quad (8)$$

Equation 9 defines heat-capacity, also known as specific-heat, as the quantity of heat per unit mass essential to rise the temperature by one unit. Calculating processing-temperatures and the amount of heat desired for processing benefits from the capacity to differentiate between two polymeric composites using specific-heat[16].

$$H = \frac{C_p}{C_v}. \quad (9)$$

RESULT AND DISCUSSION

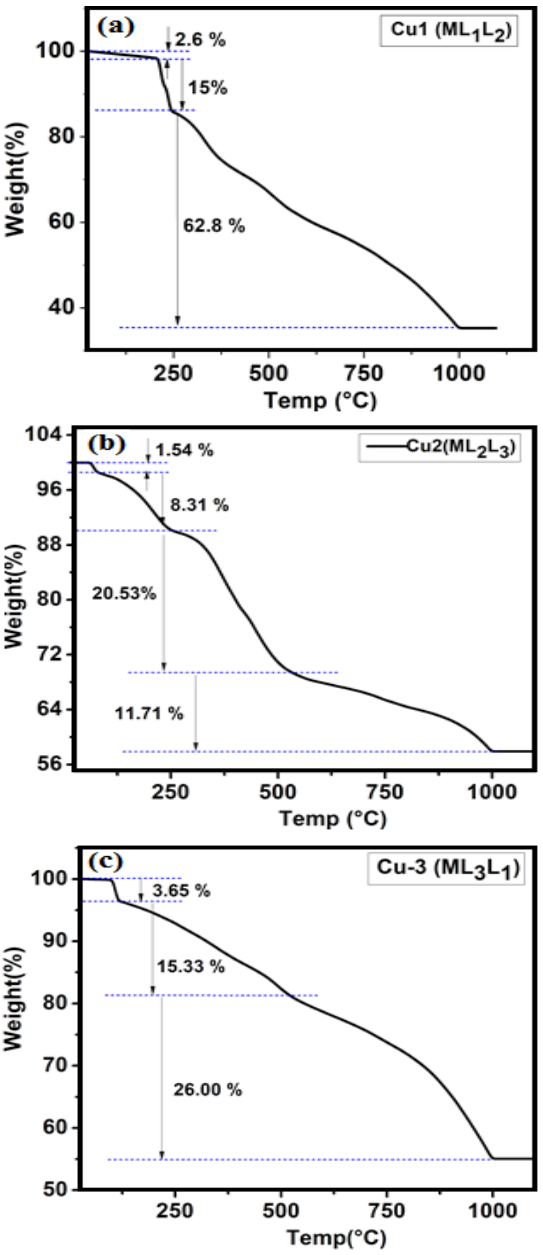

Fig. 1(a). Thermogram of $Cu(L_1L_2)$ metal complex; (b)Thermogram of $Cu(L_2L_3)$ metal complex; and (c) Thermogram of $Cu(L_3L_1)$ metal complex

Thermogram of all samples presented in Fig. 1. TGA thermogram of $Cu(L_1L_2)$ presented in Fig. 1(a), showed three weight losses. 2.6% weight loss between room temperature and 200°C, 15% loss of weight between 200°C and 250°C and 62.8% loss of weight between 250°C and 1000°C.

Four weight losses are observed in $Cu(L_2L_3)$

presented in Fig. 1(b). 1.54%, 8.31%, 20.53% and 11.71% losses found between 25°C & 75°C, 75°C & 240°C, 240°C & 530°C and 530°C& 1000°C respectively. 3.65%, 15.33%, 26% and 11.71% losses found between 25°C & 100°C, 100°C & 520°C, and 520°C & 1000°C respectively in $Cu(L_3L_1)$ presented in Fig. 1(c). the end settemperature at 801°C. The material decomposed after 1000°C in all the complexes.

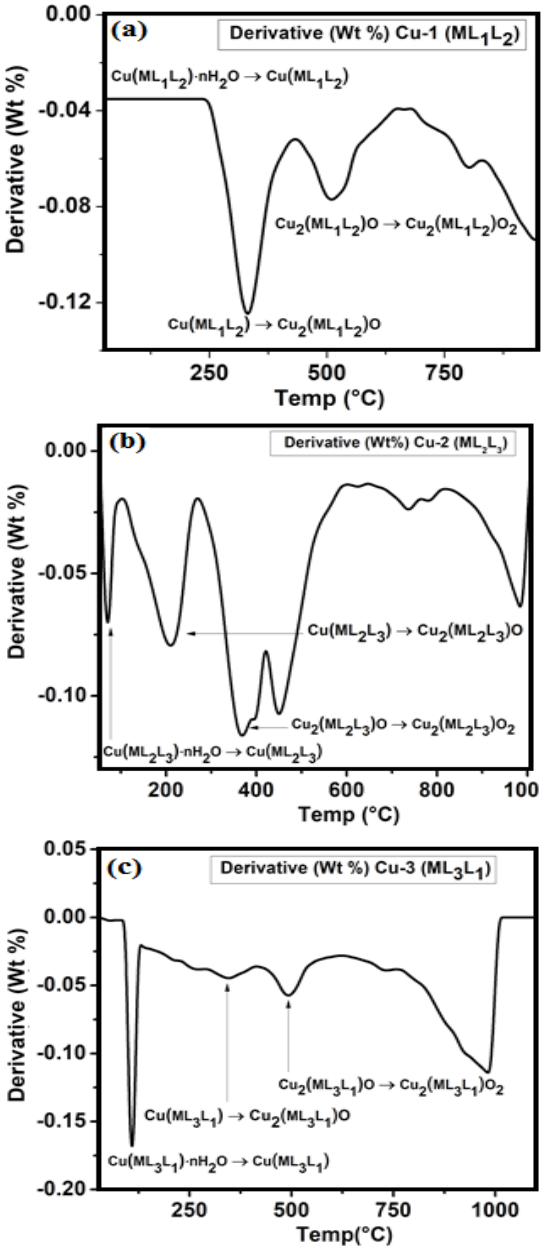

Fig. 2(a). DTG curve of $Cu(L_1L_2)$ metal complex; (b) DTG curve of $Cu(L_2L_3)$ metal complex; and (c) DTG curve of $Cu(L_3L_1)$ metal complex

Plotting the first derivative of the TGAcurvealso known as the DTG curve can help identify inflection spots that are important for differential thermal analysis and in-depth interpretations[17]. For all samples, the first derivative of weight loss with respect to temperature was computed in order to establish a chemical reaction, and it is shown in Fig. 2. The material's adsorbed surface water evaporated and became dehydrated, as evidenced by the first loss of all samples, which was noticed at 200°C for Cu-1 metal complex (Fig. 2(a)), at 75°C for Cu-2 metal complex (Fig. 2(b)) and at 100°C for Cu-3 metal complex (Fig. 2(c)). Due to phase transformation, the second and subsequent weight losses in the curve were represented by the corresponding curves[18].

To assess the kinetic parameters from the TGA curve, Broido's approach was utilized[7]. Fig. 3(a) displays plots of ln(ln 1/y) vs 1000/T (where y is the fraction that has not yet been decomposed) for the thermal degradation of metal complexes, which also illustrate the various thermal activity regions[13]. Fig. 3(b) illustrates the predicted slope of the two stages of the thermal breakdown of metal complexes.

In Table 1, the thermodynamic data were compiled. There are reactions whose rates decrease with rising temperature, as shown by the fact that activation energy Ea<0 in all complexes[19]. A chemical reaction requires a small amount of energy to proceed, as seen by the value of Ea. Enthalpy H<0, in all the mentioned compounds and heat is transferred from a system to its surroundings during the entire exothermic reaction[20]. In all complexes,entropy $\Delta S<0$ demonstrated the transformation from a less ordered state (a liquid) to a more ordered state (a crystal). In all complexes mentioned, the action is not spontaneous but instead proceeds spontaneously in the opposite direction with Gibbs energy $\Delta G>0$.[21]

Figure 4(a) illustrates the Cu-1 complex's DSC curve as temperature increases up to 1000°C. Due to a thermal event, the curve is perplexing throughout the 20°C–700°C temperature range.The complex is undergoing an endothermic process as shown by the first downward zone in the Cu-1 curve[22].

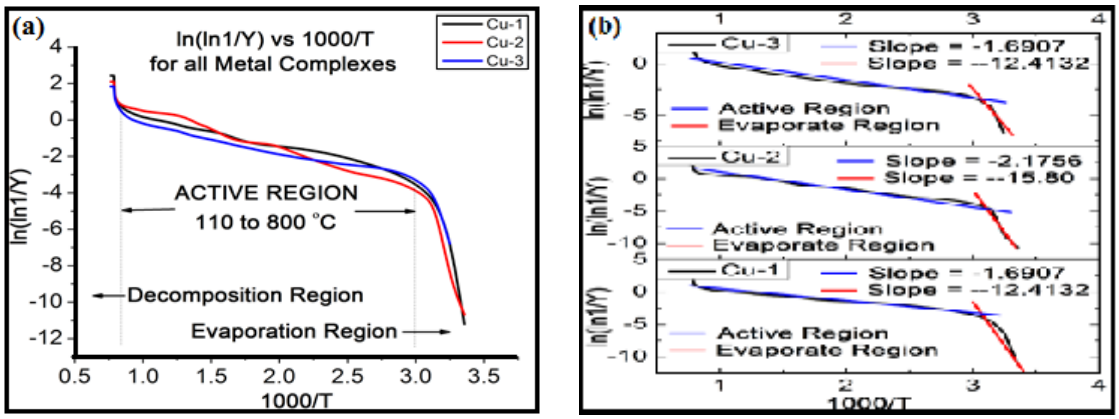

Fig. 3(a). ln(ln 1/y) versus 1000/T; and (b) Slope calculation for two stages

Table 1: Thermodynamic Parameters of all complexes

Sr. No	Material	Temp Range	R^2	Ea(kj/mol)	ΔH(kj/mol)	ΔS(J• K^{-1})	ΔG(JK^{-1} mol^{-1})
1	$Cu(L_1L_2)$	25-110	0.74908	-296.8506	-5833.97	-20.0944	7548.896
	Complex	110-800	0.96719	-32.53865	-3898.55	-18.9612	4918.406
2	$Cu(L_2L_3)$	25-110	0.82285	-302.5248	-4268.3	-19.5646	5064.024
	Complex	110-800	0.99033	-41.65652	-3076.27	-18.6641	3736.12
3	$Cu(L_3L_1)$	25-110	0.78596	-237.6773	-4120.32	-19.5374	5003.639
	Complex	110-800	0.95738	-32.37207	-2526.57	-18.1369	2914.494

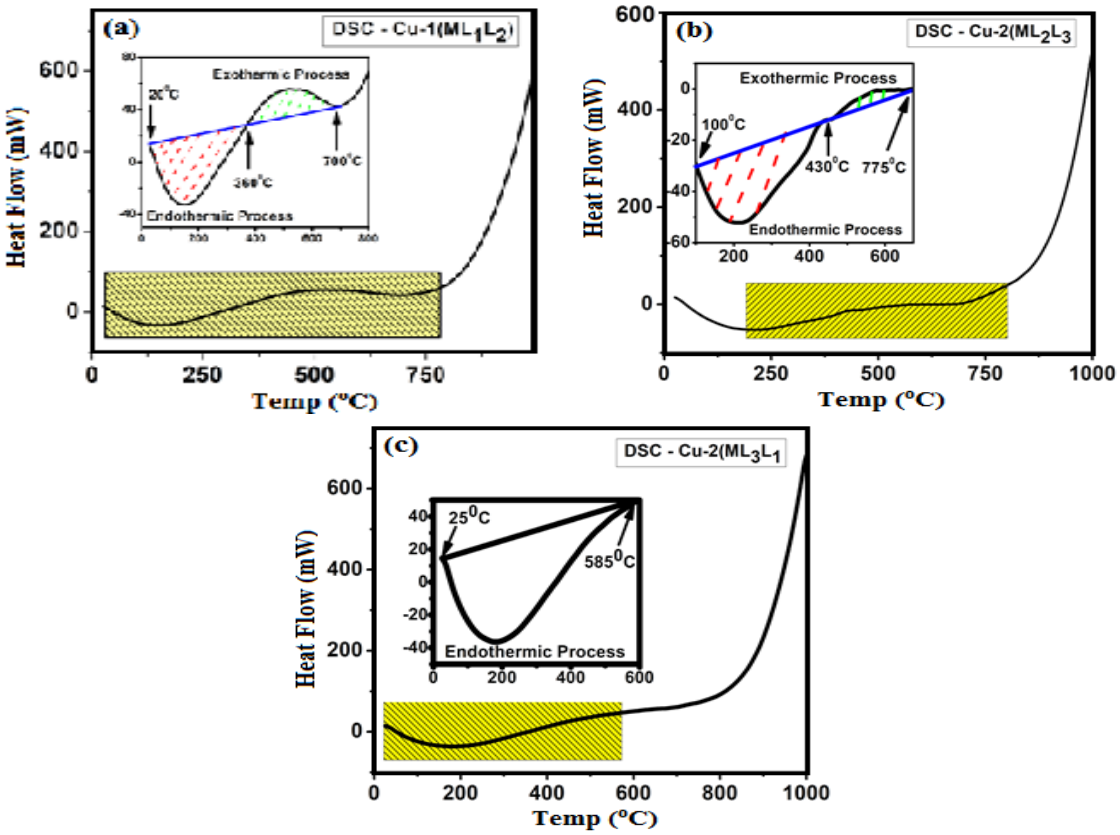

Fig. 4(a). DSC curve of $Cu(L_1L_2)$ metal complex; (b) DSC curve of $Cu(L_2L_3)$ metal complex; and (c) DSC curve of $Cu(L_3L_1)$ metal complex

The curve unmistakably demonstrates that the initial event starts at 360°C and concludes at 700°C. The melting point is 800°C, and this thermal occurrence is connected to the exothermic peak as well as the complex's breakdown. Due to a thermal event, the Cu-2 curve can be perplexing in the temperature range of 100-775°C. The Cu-2 complex curve's shown in Fig. 4(b), initial downward section denotes an endothermic crystallization process spurred on by fusion activity[23]. The curve demonstrates unequivocally that the first event starts at 430°C and concludes at 775°C. The disintegration of the Cu-2 complex, which is connected to the exothermic peak and the melting point of 700°C, is a thermal event. The Cu-3 complex curve is found in the temperature range of 25-585°C due to a thermal occurrence shown in Fig. 4(c). The only one down region in the Cu-3 curve indicates Endothermic process the complex due to fusion. The curve clearly shows that the there is no exothermic process exothermic process occurred during process[24]. The first event occurs at 585°C. The melting point is 750°C, and this thermal event is linked to the decomposition of Cu-3 complex.

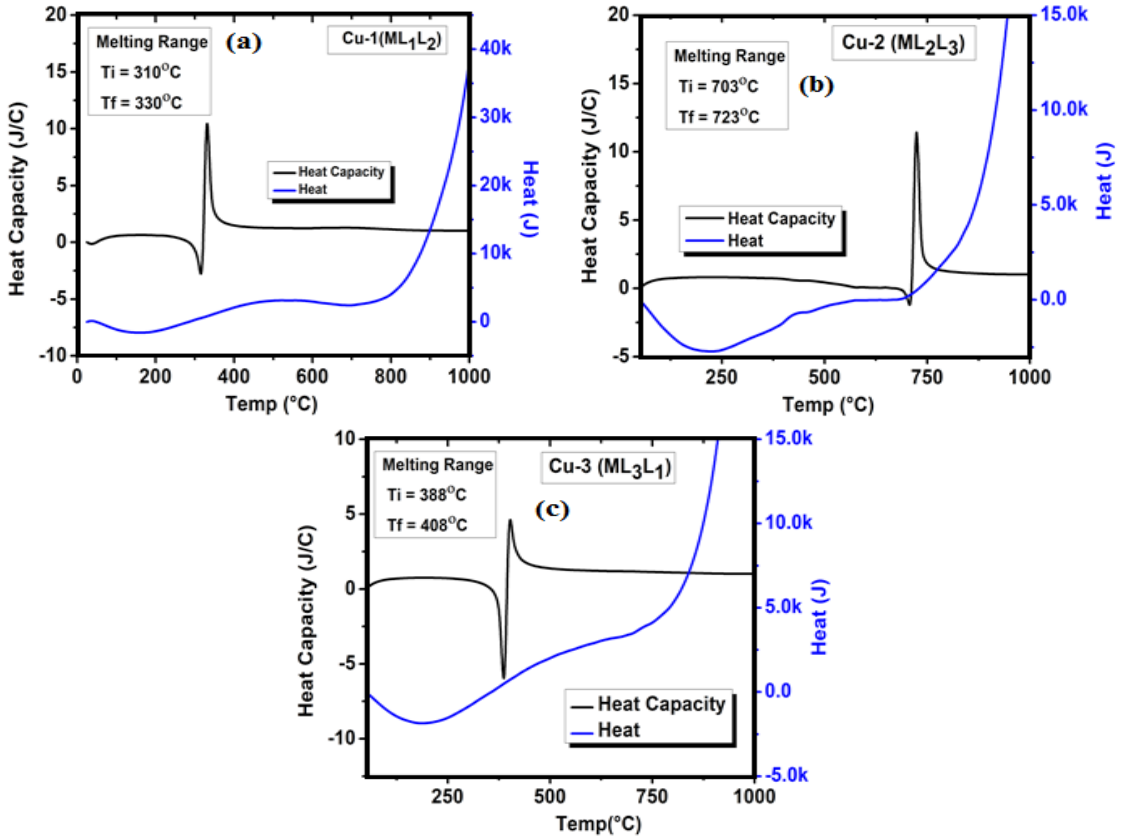

Fig. 5(a). Heat Capacity and Heat of Cu(L_1L_2) metal complex; (b) Heat Capacity and Heat of Cu(L_2L_3) metal complex; and (c) Heat Capacity and Heat of Cu(L_3L_1) metal complex

The Heat capacity and Heat variation with temperature are presented in Fig. 5 for all the complexes. From this graph the melting range Ti and Tf calculated and displayed in Table 2[25].

Table 2: Melting Range of all complexes

Sr. No	Material	Melting Range	
		Ti (°C)	Tf (°C)
1	Cu (L_1L_2)Complex	310	330
2	Cu (L_2L_3) Complex	703	723
3	Cu (L_3L_1)Complex	388	408

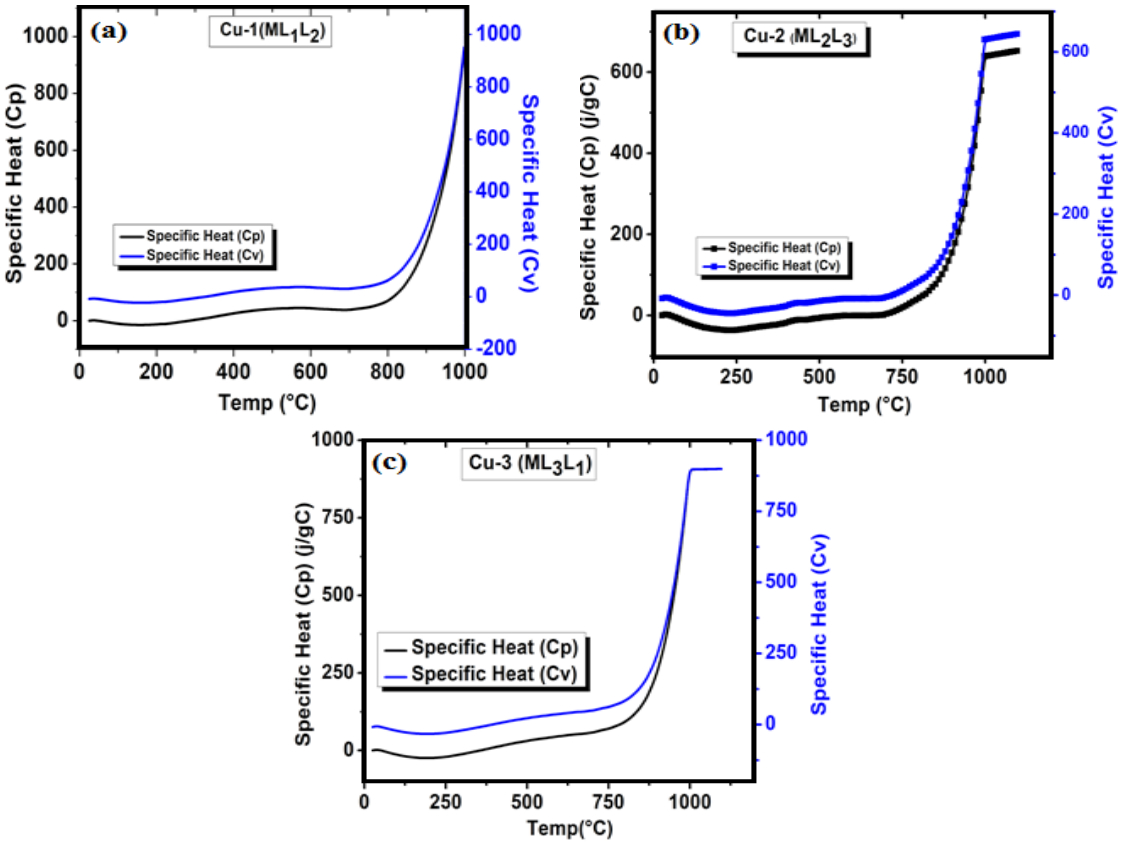

Fig. 6(a). Specific Heat of Cu(L_1L_2) metal complex; (b) Specific Heat of Cu(L_2L_1) metal complex; and (c) Specific Heat of Cu(L_3L_1) metal complex

The specific heat Cp and Cv calculated from the obtained DSC data for all complexes and presented in Fig . 6. In Cu-1 complexes the specific heat Cp and Cv remain constant up to 800°C as shown in Fig. 6(a) and after this melting point a drastically change revels the bond destruction[26]. Up to melting point 700°C the specific heat Cp and Cv remain constant in Cu-2 complex and rapidly changed after that as shown in Fig. 6(b). The rapid changed found after 750°C in specific heat Cp and Cv in Cu-3 complex presented in Figure 6(c).

CONCLUSION

The thermal degradation of CuLxLy has been examined in the present research using TGA and DSC in an inert nitrogen atmosphere. It has been discovered that pyrolysis is just one of three and four weight loss steps in the decomposition process. Dehydration occurs in the first stage at a temperature of about 100°C. The composition complexes have been discovered to be stable at high temperatures, and mass loss as a result of phase transaction with new layer-structure creation has been seen in the consequent stage. The apparent activation energy, entropy, and Gibbs free energy were derived via Broido's non-isothermal conversional approach, along with other kinetic characteristics of all metal complexes. The decomposition reaction is slow and spontaneous, as indicated by the negative Entropy and positive Gibbs free energy values. The activation energy began rapidly reducing as the entire thermal process slowed down at increasing conversions. Future objectives include gathering kinetic data using the least squares optimization method and contrasting it with the findings of this inquiry. A minuscule laboratory reactor can use kinetic parameters to characterize the pyrolysis process with good agreement. All minerals have been found to undergo an endothermic and exothermic reaction process at a particular temperature range by DSC investigation. Melting temperatures, enthalpies of fusion, and enthalpies

of crystallization are shown by the heat capacity, heat, and specific heat curve respectively.

ACKNOWLEDGMENT

This research did not receive any specific grant from funding agencies in the public, commercial, or not-for-profit sectors.

Conflict of interest

The author declare that we have no conflict of interest.

REFERENCES

1. Taboada, E.; Cabrera, G.; Jimenez, R.; Cardenas, G., *J. Appl. Polym. Sci.*, **2009**, *114*, 2043–2052 DOI 10.1002/app.30796
2. Paul, S.; Barman, P., *J. Mole. Structure.*, **2024**, *1296*, 136941.
3. Shirode, P.; Yeole, P., *Chem. Sci. Transactions.*, **2014**, *3*(3), 1186-1192.
4. Sönmez, M.; Levent, A.; Ækerci, M., *Russian J. Coordination Chem.*, **2004**, *30*, 655–660.
5. Ngo, S.; Banger, K.; DelaRosa, M.; Polyhedron, P., *J. Mole. Structure.*, **2013**, *1048*, 357-366.
6. Ferraris, J.; Balkus, K.; Schade, A., *J. Inclusion Phenomena and Mole. Recognition in Chem.*, **1992**, *14*, 163–169.
7. Broido A., *J Polym. Sci. Part A-2 Polym. Phys.*, **1969**, *7*, 1761–1773.
8. Ahmadi, R.; Molecules, S. *MDPI.Com.*, **2012**, *17*, 6434–6448.
9. Wu, K.; Wang, Y., *Poly. Degradation and Stability.*, **2003**, *79*(2), 195-200.
10. Al-Fakeh, M.; Alsikhan, M.; *Alnawmasi, J. Molecules.*, **2023**, *28*, 2555.
11. Ferrer, G.; Solé, A.; Barreneche, C.; Martorell, I.; Cabeza, L., *Renewable and Sustainable Energy Reviews.*, **2015**, *50*, 665–685.
12. McHugh, J.; Fideu, P.; Herrmann, A.; Testing, W. Elsevier., **2010**.
13. Patel, D.; Patel, K., *Mater. Today Proc.*, **2020**, *32*, 392–396.
14. Salehi, S.; Eslami, A.; Chu, Q.; Chen, D., *J Anal. Appl. Pyrolysis.*, **2024**, *178*, 106415 doi. org/10.1016/j.jaap.2024.106415
15. Mohammad, N.; Fawwaz K.; Shrafat's, D.; Sweileh, A., *Sustainable Env.*, **2024**, *10*, 2024.
16. Scuiller, E.; Dutournié, P.; Zbair, M.; Bennici, S., *J Chem. Eng. Data.*, **2023**, *68*, 1865–1871.
17. Saadatkhah, N.; Carillo, A.; Ackermann, S.; Leclerc, P.; Latifi, M.; Samih, S.; Patience, S.; Chaouki, J. Can., *J. Chem. Eng.*, **2020**, *98*, 34–43.
18. Aly, A.; Hassan, S.; El-Boraey, A.; Eldourghamy, A.; Abdalla, M.; Alminderej, M.; Elganzory, H., *Arab. J. Sci. Eng.*, **2024**, *49*, 361–379.
19. Karbasi, A.; Darvishi, R.; Gerdroodbar, A.; Payam, G., *Int. J.Polym. Sci.*, **2023**, 2023.
20. Dafa, T.; Wuana, A.; Iornumbe, N.; Tivkaa, T., *Chem. Search Journal.,* **2023**, *14*, 46–57.
21. Zhang, M.; Zhang, W.; Liang, G., *Eur. J.Inorg. Chem.*, **2023**, *26*, e202300183.
22. Xu, Y.; Wang, Y.; Zhong, Y.; Lei, G.; Li, Z.; Zhang, J.; Zhang, T., *Energy and Fuels.*, **2020**, *34*, 14667–14675.
23. Sekerci, M.; Yakuphanoglu, F., *J. Therm. Anal. Calorim.*, **2004**, *75*, 189–195.
24. Revanth, J.; Madhav, V.; Kalyan, Y.; Krishna, D.; Srividya, K.; Sumanth, H., *Mater. Today Proc.*, **2020**, *26*, 460–465.
25. Ozen, M.; Demircan, G.; Kisa, M.; Acikgoz, A.; Ceyhan, G.; IÆker, Y., *Mater. Chem. Phys.*, **2022**, 278.
26. Saxena, P.; Shukla, P.; Gaur, M., *Poly. and Poly. Compo.*, **2021**, *29*, S11–S18.